Fluctuation and noise propagation in phenotypic transition cascades of clonal populations

Qi-ming Pei,[1,2] Xuan Zhan,[1,*] Li-jian Yang,[1] Jian Shen,[1] Li-fang Wang,[1] Kang Qui,[1] Ting Liu,[1] J. B. Kirunda,[1] A. A. M. Yousif,[1] An-bang Li,[1] and Ya Jia[1,†]

[1]*Institute of Biophysics and Department of Physics, Central China Normal University, Wuhan 430079, China*

[2]*School of Physics and Optoelectronic Engineering, Yangtze University, Jingzhou 434023, China*

(Received 3 February 2015; revised manuscript received 22 April 2015; published 29 July 2015)

Quantitative modeling of fluctuations of each phenotype is a crucial step towards a fundamental understanding of noise propagation through various phenotypic transition cascades. The theoretical formulas for noise propagation in various phenotypic transition cascades are derived by using the linear noise approximation of master equation and the logarithmic gain. By virtue of the theoretical formulas, we study the noise propagation in bidirectional and unidirectional phenotypic transition cascades, respectively. It is found that noise propagation in these two phenotypic transition cascades evidently differs: In the bidirectional cascade, a systemic random environment is provided by a correlated global component. The total noise of each phenotype is mainly determined by the intrinsic noise and the transmitted noise from other phenotypes. The intrinsic noise enlarged by interconversion through an added part shows a novel noise propagation mechanism. However, in the unidirectional cascade, the random environment of each downstream phenotype is provided by upstream phenotypes. The total noise of each downstream phenotype is mainly determined by the transmitted noises from upstream phenotypes. The intrinsic noise and the conversion noise can propagate in both bidirectional and unidirectional phenotypic transition cascades.

DOI: 10.1103/PhysRevE.92.012721 PACS number(s): 87.18.Tt, 05.40.−a, 87.10.Mn, 87.23.−n

I. INTRODUCTION

Phenotypic diversity exists in a variety of species, from unicellular organisms such as *Salmonella enterica* [1], *Escherichia coli* [2], or *Bacillus subtilis* [3] to plants [4] and animals [5]. Many previous research works about cellular phenotypic diversity refer to the stochastic cell fate decisions modulated by random gene expressions [6–9] or generated by environmental changes [2,10–13]. Under fixed physiological conditions, however, the interconversion between distinct phenotypes which can constitute various phenotypic transition cascades [14,15] or the self-proliferation of each phenotype can maintain phenotypic equilibrium in clonal populations. For instance, phenotypic equilibrium is observed in various cancer cells in distinct states in *in vivo* and *in vitro* cultures [16,17]. The phenotypic transition processes around the equilibrium state may be hindered by stochastic fluctuations arising from the variations of interconversion or self-proliferation rate.

A significant problem in populations is to understand how noise propagates in various phenotypic transition cascades around the equilibrium state. Similar problems were investigated in some biological cascades or network systems. For example, ultrasensitive signaling cascades operating near saturation show that output signal fluctuations are bounded in magnitude even if the noisy cascade length is large and the noise in these fluctuation-bounded cascades can be attenuated [18]. A gene-regulatory network of single cells [19] explains the noise propagation through the gene network and predicts the correlations as the network is systematically perturbed. In gene regulation in terms of a two-state model, where the promoter of a gene can stochastically switch between an on and an off state, noise in gene expression to promoters described by state transition diagrams with multiple states, the experimentally accessible noise characteristics for these complex promoters, and the channel capacities of complex promoter architectures are studied in detail, respectively [20]. It was found that adding internal states to the promoter can generically decrease the channel capacity, except in certain cases. A network of interactions between genes and proteins [21] shows that the positive feedback as a central motif allows for the buffering of propagated noise while maintaining sensitivity to long-term changes in input signals.

In order to investigate noise propagation through various phenotypic transition cascades, in this paper we start by constructing a general model of populations in which the conversion rate between distinct phenotypes and the self-proliferation rate of each phenotype are assumed as arbitrary functions of subpopulations. The theoretical formulas for noise propagation in phenotypic transition cascades are derived by using the linear noise approximation of a master equation [22,23]. The theoretical formulas for noise propagation obtained here can be widely applied to investigate the fluctuations and noise propagation in various phenotypic transition cascades (or interaction networks).

To maintain the phenotypic equilibrium, there are two regulation mechanisms: First, the phenotypic equilibrium can be maintained through intercellular signals that modulate the proliferation rates of distinct states in the absence of interconversion between two states. Second, the phenotypic states can interconvert between different states in a manner that maintains phenotype equilibrium in the absence of proliferation rate variations. On the other hand, there are two conceivable phenotypic transition ways. One is the bidirectional transition cascade, such as the transitions between two species in a bacterial community with exploitative competition [24] and the interconversion between three cell states in breast cancer lines [16]. The other is the unidirectional transition cascade,

*zhanx@phy.ccnu.edu.cn
†jiay@phy.ccnu.edu.cn

such as the differentiation from stem cell to semidifferentiated cell and then to fully differentiated cell in a colonic crypt [17].

Interesting questions now arise: How does noise propagate in bidirectional and unidirectional transition cascades respectively? What are the effects of the interconversion or self-proliferation rates of one phenotype on noise propagation in the two phenotypic transition cascades around the equilibrium state? To address these issues, by virtue of our theoretical formulas for noise propagation in transition cascades, we study a model of two species with exploitative competition in a bacterial community [24], which is a case of the bidirectional phenotypic transition cascade with the first regulation mechanism, and a model of three cell compartments in a colonic crypt [17], which is a case of the unidirectional phenotypic transition cascade with the second regulation mechanism, respectively. We found that both the mechanisms of noise propagation and the effects of the interconversion or self-proliferation rate on noise propagation significantly differ in the bidirectional and unidirectional transition cascades.

The paper is arranged as follows. We start by constructing a general model of populations in which the conversion rates between distinct phenotypes and the self-proliferation rate of each phenotype are assumed as arbitrary functions of subpopulations in Sec. II, and the variances and covariances of fluctuations are obtained by using the linear noise approximation of the master equation [22,23]. In Sec. III, the theoretical formulas for noise propagation in phenotypic transition cascades are derived by using the logarithmic gain [19,21,25–27]. By virtue of these theoretical formulas, the fluctuations and noise propagation in a bidirectional [24] and in unidirectional [17] phenotypic transition cascades are respectively studied in Secs. IV and V. We end with conclusions and discussions in Sec. VI.

II. GENERAL MODEL

We consider a general phenotypic transition cascade model with R phenotypes and L transitions that encompasses both self-proliferation and transition from one phenotypic state to another. The subpopulation kinetics of population vector $\mathbf{N}(t) = [N_1(t), N_2(t), \ldots, N_R(t)]$ is given by allowing it to change with time in accordance with self-proliferation, death, and phenotypic transitions among different phenotypes:

$$\frac{dN_i}{dt} = a_i N_i - b_i N_i + \sum_{j\neq i} \alpha_{ji} N_j - \sum_{j\neq i} \alpha_{ij} N_i, \qquad (1)$$

where a_i and b_i are the self-proliferation and death rates of the ith phenotype and α_{ij} is the interconversion rate between the ith and the jth phenotypes.

In general, all rates in Eq. (1) depend on the number of involved phenotypes. Here we assume that (i) the self-proliferation (or self-growth) rates are arbitrary functions of subpopulations in the form of $a_i = a_i(g_i, N_i, N_j)$ with a maximal growth rate (MGR) g_i, e.g., the logistic growth fashion in the bacterial competition strategies of two species community due to the limited nutrition [12,24]. (ii) The conversion rates are arbitrary functions of subpopulations in the form of $\alpha_{ij} = \alpha_{ij}(s_i, N_i, N_j)$ with an inherent transition rate (ITR) s_i, e.g., the linear feedback or the saturating feedback mechanism of transition between three cell phenotypes in a colonic crypt [17,28]. (iii) The death rate b_i of each phenotype is considered a constant here.

The joint probability distribution $P(N_1, N_2, \ldots, N_R, t)$ of population kinetics Eq. (1) obeys the following master equation [22,23,29]:

$$\frac{\partial P}{\partial t} = \sum_{i=1}^{R} \Big[\big(\mathbb{E}_i^{-1} - 1\big) a_i N_i + \big(\mathbb{E}_i^{1} - 1\big) b_i N_i + \sum_{j\neq i} \big(\mathbb{E}_j^{1}\mathbb{E}_i^{-1} - |, 1\big) \alpha_{ji} N_j + \sum_{j\neq i} \big(\mathbb{E}_i^{1}\mathbb{E}_j^{-1} - 1\big) \alpha_{ij} N_i \Big] P, \qquad (2)$$

where $\mathbb{E}_i$ and $\mathbb{E}_j$ are the step operators acting on N_i and N_j, respectively. For a function $f(N_i, N_j)$ with two integer arguments, the step operator $\mathbb{E}_i^{\pm m}$ (or $\mathbb{E}_j^{\pm m}$) increases N_i (N_j) by an integer $\pm m$, i.e., $\mathbb{E}_i^{\pm m} f(N_i, N_j) = f(N_i \pm m, N_j)$, $\mathbb{E}_j^{\pm m} f(N_i, N_j) = f(N_i, N_j \pm m)$.

The master equation cannot be solved exactly, so it is necessary to have a systematic approximation method. By using van Kampen's Ω-expansion method [22], the subpopulation is approximated by setting $N_i(t) = \Omega x_i(t) + \sqrt{\Omega}\xi_i(t)$ for large system size Ω, and the joint probability distribution is written by $P(N_1, N_2, \ldots, N_R, t) = \Omega^{-R/2}\Pi(\xi_1, \xi_2, \ldots, \xi_R, t)$. Collecting the terms of $\Omega^{1/2}$ in the expansion of Eq. (2) reproduces the concentration form of the macroscopic rate equation,

$$\frac{dx_i}{dt} = a_i x_i - b_i x_i + \sum_{j\neq i} \alpha_{ji} x_j - \sum_{j\neq i} \alpha_{ij} x_i, \qquad (3)$$

and the terms of Ω^0 form a linear Fokker-Planck equation,

$$\frac{\partial}{\partial t}\Pi = -\sum_{i,k}^{R} A_{ik} \frac{\partial}{\partial \xi_i}(\xi_k \Pi) + \frac{1}{2}\sum_{i,k}^{R} B_{ik} \frac{\partial^2 \Pi}{\partial \xi_i \partial \xi_k}, \qquad (4)$$

where $\mathbf{A}$ is the drift matrix and $\mathbf{B}$ is the diffusion matrix. $\mathbf{A}$ and $\mathbf{B}$ depend on the stoichiometry of the transitions and the macroscopic rates.

Under the steady state $(x_1^s, x_2^s, \ldots, x_R^s)$ of the macroscopic rate Eq. (3), the matrix elements of $\mathbf{A}$ and $\mathbf{B}$ in Eq. (4) are defined by

$$A_{ik} = \sum_{l=1}^{L} s_{il} \frac{\partial \upsilon_l}{\partial x_k}, \quad B_{ik} = \sum_{l=1}^{L} s_{il} s_{kl} \upsilon_l,$$

in which the transition l occurs with the microscopic rate υ_l to produce subpopulation s_{il} of phenotype i and subpopulation s_{kl} of phenotype k. Taking into account Eq. (3), we have the expressions for matrix elements A_{ik} and B_{ik} as follows:

$$A_{ii} = \frac{\partial}{\partial x_i}\left(a_i x_i - b_i x_i - \sum_{j\neq i} \alpha_{ij} x_i\right), \qquad (5)$$

$$A_{ik} = \frac{\partial}{\partial x_k}(a_i x_i - b_i x_i + \alpha_{ki} x_k), \qquad (6)$$

$$B_{ii} = 2\left(a_i x_i + \sum_{j\neq i} \alpha_{ji} x_j\right), \qquad (7)$$

$$B_{ik} = -(\alpha_{ik} x_i + \alpha_{ki} x_k), \qquad (8)$$

with $k \neq i$. For stationary variances, the linear noise approximation is summarized by [30,31]

$$\mathbf{AC} + \mathbf{CA}^{\mathbf{T}} + \Omega\mathbf{B} = 0, \tag{9}$$

where matrix $\mathbf{C}$ contains both the variance C_{ii} which characterizes the fluctuation in population of the ith phenotype and the covariance C_{ik} which represents the degree of correlation between the noise in the ith subpopulation and that in the kth subpopulation. Substituting Eqs. (5)–(8) into Eq. (9), the variances C_{ii} and covariances C_{ik} of the fluctuations are obtained as

$$C_{ii} = \frac{\sum_{j\neq i} C_{ij}\frac{\partial}{\partial x_j}(a_i x_i - b_i x_i + \alpha_{ji}x_j) + \Omega\left(a_i x_i + \sum_{j\neq i}\alpha_{ji}x_j\right)}{\frac{1}{x_i}\sum_{j\neq i}\alpha_{ji}x_j - x_i\frac{\partial}{\partial x_i}\left(a_i - b_i - \sum_{j\neq i}\alpha_{ij}\right)}, \tag{10}$$

$$C_{ik} = \frac{\sum_{j\neq k} C_{ij}\frac{\partial}{\partial x_j}(a_k x_k - b_k x_k + \alpha_{jk}x_j) + \sum_{j\neq i} C_{kj}\frac{\partial}{\partial x_j}(a_i x_i - b_i x_i + \alpha_{ji}x_j) - \Omega\left(\alpha_{ik}x_i + \alpha_{ki}x_k\right)}{\frac{1}{x_i}\sum_{j\neq i}\alpha_{ji}x_j + \frac{1}{x_k}\sum_{j\neq k}\alpha_{jk}x_j - x_i\frac{\partial}{\partial x_i}\left(a_i - b_i - \sum_{j\neq i}\alpha_{ij}\right) - x_k\frac{\partial}{\partial x_k}\left(a_k - b_k - \sum_{j\neq k}\alpha_{kj}\right)}, \quad \text{for} \quad k \neq i. \tag{11}$$

III. THEORETICAL FORMULAS FOR NOISE PROPAGATION

To quantify the noise propagation in phenotypic transition cascades around the steady state, Eq. (9) is normalized as

$$\mathbf{MV} + (\mathbf{MV})^{\mathbf{T}} + \mathbf{D} = 0, \tag{12}$$

with

$$V_{ik} = V_{ki} = \frac{C_{ik}}{\langle N_i\rangle\langle N_k\rangle}, \quad M_{ik} = A_{ik}\frac{\langle N_k\rangle}{\langle N_i\rangle}, \quad D_{ik} = \frac{\Omega B_{ik}}{\langle N_i\rangle\langle N_k\rangle}.$$

By using Eqs. (7) and (8) and $N_i(t) = \Omega x_i(t) + \sqrt{\Omega}\xi_i(t)$, we have

$$D_{ii} = \frac{2\left[a_i\langle N_i\rangle + \sum_{j\neq i}\alpha_{ji}\langle N_j\rangle\right]}{\langle N_i\rangle^2}, \tag{13}$$

$$D_{ik} = -\left(\frac{\alpha_{ik}}{\langle N_k\rangle} + \frac{\alpha_{ki}}{\langle N_i\rangle}\right), \quad \text{with} \quad k \neq i. \tag{14}$$

To measure how the balance between production and elimination of N_i is affected by N_k, the logarithmic gain [19,21,25–27] is defined by

$$H_{ik} = \frac{\partial \ln(J_i^-/J_i^+)}{\partial \ln(N_k)},$$

where $J_i^+ = a_i N_i + \sum_{j\neq i}\alpha_{ji}N_j$ is the pure production rate of phenotype i and $J_i^- = b_i N_i + \sum_{j\neq i}\alpha_{ij}N_i$ is the pure elimination rate of phenotype i. In fact, H_{ik} represents a common measure of the sensitivity of a response to variation in parameter N_k, which is also called the logarithmic gain [32], sensitivity amplification [33,34], or susceptibility [35]. Taking into account the population kinetics [Eq. (1)], we have

$$H_{ii} = \frac{\sum_{j\neq i}\alpha_{ji}N_j + N_i^2\frac{\partial}{\partial N_i}\left(b_i - a_i + \sum_{j\neq i}\alpha_{ij}\right)}{a_i N_i + \sum_{j\neq i}\alpha_{ji}N_j}, \tag{15}$$

$$H_{ik} = \frac{N_i}{a_k N_k + \sum_{j\neq k}\alpha_{jk}N_j}\frac{\partial}{\partial N_i}(b_k N_k - a_k N_k - \alpha_{ik}N_i), \quad \text{for} \quad k \neq i. \tag{16}$$

Under the steady state (i.e., $J_i^+ = J_i^- = J_i$), the average lifetime is determined by the subpopulation divided by the total rate of elimination, $\tau_i = N_i/J_i^- = N_i/J_i$. Thus, the drift matrix $\mathbf{A}$ is rewritten as

$$A_{ik} = -\frac{\langle N_i\rangle}{\langle N_k\rangle}\frac{H_{ki}}{\tau_i}.$$

Then its normalized formation $\mathbf{M}$ is represented by

$$M_{ik} = A_{ik}\frac{\langle N_k\rangle}{\langle N_i\rangle} = -\frac{H_{ki}}{\tau_i}. \tag{17}$$

Substituting Eqs. (13), (14), and (17) into Eq. (12), we obtain

$$\sum_{j=1}^{R} H_{ji}V_{ji} = \frac{1}{\langle N_i\rangle}, \tag{18}$$

$$\sum_{j=1}^{R}\left(\frac{H_{ji}V_{jk}}{\tau_i} + \frac{H_{jk}V_{ji}}{\tau_k}\right) = -\left(\frac{\alpha_{ik}}{\langle N_k\rangle} + \frac{\alpha_{ki}}{\langle N_i\rangle}\right), \tag{19}$$

with $k \neq i$.

The solution V_{ii} of the theoretical formulas Eqs. (18) and (19) represents the total noise in the ith phenotypic state, which may include the intrinsic noise in the ith phenotypic state, the transmitted noise from the other phenotypes, and the interconversion noise. The solution V_{ij} represents the correlation between fluctuations in the ith phenotype and in the jth phenotype. By virtue of above theoretical formulas one can investigate fluctuations and noise propagation in various transition cascades (or networks) around equilibrium state when the conversion rates between distinct phenotypes and the self-proliferation rate of each phenotype are provided.

In order to study how the noise propagates in various phenotypic transition cascades and the effects of the interconversion rates or self-proliferation rates on noise propagation in phenotypic transition cascades, under given detailed expressions of the conversion rates and the self-proliferation rate, we discussed a model of two species with exploitative competition in a bacterial community [24], which is a case of the bidirectional phenotypic transition cascade with the first regulation mechanism, and a model of three cell compartments in a colonic crypt [17], which is a case of the unidirectional phenotypic transition cascade with the second regulation mechanism in Secs. IV and V, respectively.

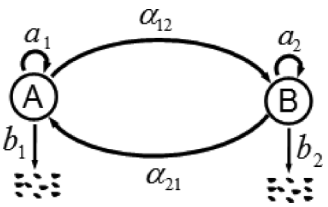

FIG. 1. The bidirectional phenotypic transition cascade. A schematic diagram of transitions between species A and species B in bacterial community.

IV. FLUCTUATIONS AND NOISE PROPAGATION IN THE BIDIRECTIONAL TRANSITION CASCADE

A. Model and noise propagation formulae

Consider a model of a bacterial community (including species A and species B) with exploitative competition [24]. This is a case of bidirectional phenotypic transition cascade (see Fig. 1) with the first regulation mechanism. In the deterministic description, the evolution functions are

$$\frac{dN_1}{dt} = a_1N_1 - b_1N_1 + \alpha_{21}N_2 - \alpha_{12}N_1, \tag{20}$$

$$\frac{dN_2}{dt} = a_2N_2 - b_2N_2 + \alpha_{12}N_1 - \alpha_{21}N_2, \tag{21}$$

where N_1 and N_2 are the population numbers of species A and B. In this model, the self-proliferation rates of two species are $a_1 = g_1[1-(N_1+N_2)/N_0]$ with MGR g_1 and $a_2 = g_2[1-(N_1+N_2)/N_0]$ with MGR g_2, in which N_0 refers to the carrying capacity of the community constrained by nutrient limitation. The ITRs between different phenotypes are $s_1 = \alpha_{12}$ and $s_2 = \alpha_{21}$, respectively. It is the classical competitive Lotka-Volterra equations [36–38] when $\alpha_{12} = \alpha_{21} = 0$. Here we take the dimensionless parameters $g_2 = 0.121$, $\alpha_{21} = 0.001$, and $b_1 = b_2 = 0.02$ [12,24].

The concentration forms of the macroscopic rate equations Eqs. (20) and (21) are

$$\frac{dx_1}{dt} = a_1x_1 - b_1x_1 + \alpha_{21}x_2 - \alpha_{12}x_1, \tag{22}$$

$$\frac{dx_2}{dt} = a_2x_2 - b_2x_2 + \alpha_{12}x_1 - \alpha_{21}x_2. \tag{23}$$

The steady state can be obtained as follows:

$$N_1^s = \Omega x_1^s = \frac{\rho_1\beta_2 + \alpha_{12}}{g_2}\frac{N_0}{\rho_1(1+\rho_1)}, \tag{24}$$

$$N_2^s = \Omega x_2^s = \frac{\rho_1\beta_2 + \alpha_{12}}{g_2}\frac{N_0}{1+\rho_1}, \tag{25}$$

with

$$\beta_1 = g_1 - b_1 - \alpha_{12},$$

$$\beta_2 = g_2 - b_2 - \alpha_{21},$$

$$\rho_1 \equiv \frac{N_2^s}{N_1^s} = \frac{g_1\beta_2 - g_2\beta_1 + \sqrt{(g_1\beta_2 - g_2\beta_1)^2 + 4g_1g_2\alpha_{12}\alpha_{21}}}{2g_2\alpha_{21}}.$$

Here β_1 and β_2 denote the inherent net (per-capita) growth rates of two species, respectively. ρ_1 is the ratio of the population of species B to that of species A.

Because the death rates $b_i (i = 1,2)$ and the transition rates $\alpha_{ij}(i, j = 1,2)$ are constant in this model, Eqs. (10) and (11) can be simplified as

$$C_{ii} = \frac{\sum_{j\neq i} C_{ij}\left(\alpha_{ji} + x_i\frac{\partial}{\partial x_j}a_i\right) + \Omega\left(a_ix_i + \sum_{j\neq i}\alpha_{ji}x_j\right)}{\frac{1}{x_i}\sum_{j\neq i}\alpha_{ji}x_j - x_i\frac{\partial}{\partial x_i}a_i},$$

$$C_{ik} = \frac{\sum_{j\neq k} C_{ij}\left(\alpha_{jk} + x_k\frac{\partial}{\partial x_j}a_k\right) + \sum_{j\neq i} C_{kj}\left(\alpha_{ji} + x_i\frac{\partial}{\partial x_j}a_i\right) - \Omega(\alpha_{ik}x_i + \alpha_{ki}x_k)}{\frac{1}{x_i}\sum_{j\neq i}\alpha_{ji}x_j + \frac{1}{x_k}\sum_{j\neq k}\alpha_{jk}x_j - x_i\frac{\partial}{\partial x_i}a_i - x_k\frac{\partial}{\partial x_k}a_k}, \quad \text{for} \quad k \neq i.$$

The stationary population number can be replaced by its mean number, i.e., $N_i^s \equiv \langle N_i\rangle (i = 1,2)$. From the macroscopic description of Eqs. (22) and (23), we obtain

$$C_{11} = \frac{a_1\langle N_1\rangle + \alpha_{21}\langle N_2\rangle + (\alpha_{21} - \rho_2\langle N_1\rangle)C_{12}}{\rho_1\alpha_{21} + \rho_2\langle N_1\rangle}, \tag{26}$$

$$C_{22} = \frac{a_2\langle N_2\rangle + \alpha_{12}\langle N_1\rangle + (\alpha_{12} - \rho_3\langle N_2\rangle)C_{12}}{\alpha_{12}/\rho_1 + \rho_3\langle N_2\rangle}, \tag{27}$$

$$C_{12} = C_{21} = \frac{\frac{(\alpha_{21}-\rho_2\langle N_1\rangle)(a_2\langle N_2\rangle+\alpha_{12}\langle N_1\rangle)}{\alpha_{12}/\rho_1+\rho_3\langle N_2\rangle} + \frac{(\alpha_{12}-\rho_3\langle N_2\rangle)(a_1\langle N_1\rangle+\alpha_{21}\langle N_2\rangle)}{\rho_1\alpha_{21}+\rho_2\langle N_1\rangle} - (\alpha_{12}\langle N_1\rangle + \alpha_{21}\langle N_2\rangle)}{\alpha_{12}/\rho_1 + \rho_3\langle N_2\rangle + \rho_1\alpha_{21} + \rho_2\langle N_1\rangle - \frac{(\alpha_{12}-\rho_3\langle N_2\rangle)(\alpha_{21}-\rho_2\langle N_1\rangle)}{\alpha_{12}/\rho_1+\rho_3\langle N_2\rangle} - \frac{(\alpha_{12}-\rho_3\langle N_2\rangle)(\alpha_{21}-\rho_2\langle N_1\rangle)}{\rho_1\alpha_{21}+\rho_2\langle N_1\rangle}}. \tag{28}$$

Considering the constant death rates $b_i (i = 1,2)$ and the constant transition rates $\alpha_{ij}(i, j = 1,2)$, Eqs. (15) and (16) can be simplified as

$$H_{ii} = \frac{\sum_{j\neq i}\alpha_{ji}N_j - N_i^2\frac{\partial}{\partial N_i}a_i}{a_iN_i + \sum_{j\neq i}\alpha_{ji}N_j},$$

$$H_{ik} = -\frac{N_i}{a_kN_k + \sum_{j\neq k}\alpha_{jk}N_j}\frac{\partial}{\partial N_i}(a_kN_k + \alpha_{ik}N_i), \quad \text{for} \quad k \neq i.$$

Therefore,

$$H_{11} = \frac{\rho_1\alpha_{21} + \rho_2\langle N_1\rangle}{a_1 + \rho_1\alpha_{21}}, \tag{29}$$

$$H_{22} = \frac{\alpha_{12}/\rho_1 + \rho_3\langle N_2\rangle}{a_2 + \alpha_{12}/\rho_1}, \tag{30}$$

$$H_{12} = \frac{\rho_3\langle N_2\rangle - \alpha_{12}}{\rho_1 a_2 + \alpha_{12}}, \tag{31}$$

$$H_{21} = \frac{\rho_2\langle N_1\rangle - \alpha_{21}}{a_1/\rho_1 + \alpha_{21}}. \tag{32}$$

Here $\rho_2 = g_1/N_0$ and $\rho_3 = g_2/N_0$. It can be shown that the logarithmic gains are $H_{11}, H_{22}, H_{12} > 0$ if $g_1 \in [0,0.24]$, $H_{21} \leqslant 0$ if $g_1 \in [0,0.022]$, and $H_{21} > 0$ if $g_1 \in (0.022,0.24]$.

In order to study noise propagation in species A and B, expanding the theoretical formulas Eqs. (18) and (19) and solving them for V_{11}, V_{12}, V_{21}, and V_{22} here, we have

$$V_{11} = \frac{1}{\langle N_1\rangle H_{11}} - V_{12}\frac{H_{21}}{H_{11}}, \tag{33}$$

$$V_{22} = \frac{1}{\langle N_2\rangle H_{22}} - V_{21}\frac{H_{12}}{H_{22}}, \tag{34}$$

$$V_{12} = V_{21} = -\frac{\frac{H_{12}}{\tau_2}\frac{1}{\langle N_1\rangle H_{11}} + \frac{H_{21}}{\tau_1}\frac{1}{\langle N_2\rangle H_{22}} + \frac{\alpha_{12}}{\langle N_2\rangle} + \frac{\alpha_{21}}{\langle N_1\rangle}}{\frac{H_{11}}{\tau_1} + \frac{H_{22}}{\tau_2} - \frac{H_{21}}{\tau_1}\frac{H_{12}}{H_{22}} - \frac{H_{12}}{\tau_2}\cdot\frac{H_{21}}{H_{11}}}, \tag{35}$$

where the average lifetimes are $\tau_1 = 1/(b_1 + \alpha_{12})$, $\tau_2 = 1/(b_2 + \alpha_{21})$, respectively. Thus,

$$V_{11} = \overbrace{\underbrace{\frac{1}{\langle N_1\rangle H_{11}}}_{Pure} + \underbrace{\frac{H_{21}}{H_{11}}\frac{H_{12}}{\tau_2}\epsilon\frac{1}{\langle N_1\rangle H_{11}}}_{Added}}^{Intrinsic\ noise\ in\ species\ A} + \overbrace{\frac{H_{21}}{H_{11}}\frac{H_{21}}{\tau_1}\epsilon\frac{1}{\langle N_2\rangle H_{22}}}^{Transmitted\ noise\ from\ species\ B} + \overbrace{\frac{H_{21}}{H_{11}}\epsilon\left(\frac{\alpha_{12}}{\langle N_2\rangle} + \frac{\alpha_{21}}{\langle N_1\rangle}\right)}^{interconversion\ noise}, \tag{36}$$

$$V_{22} = \overbrace{\underbrace{\frac{1}{\langle N_2\rangle H_{22}}}_{Pure} + \underbrace{\frac{H_{12}}{H_{22}}\frac{H_{21}}{\tau_1}\epsilon\frac{1}{\langle N_2\rangle H_{22}}}_{Added}}^{Intrinsic\ noise\ in\ species\ B} + \overbrace{\frac{H_{12}}{H_{22}}\frac{H_{12}}{\tau_2}\epsilon\frac{1}{\langle N_1\rangle H_{11}}}^{Transmitted\ noise\ from\ species\ A} + \overbrace{\frac{H_{12}}{H_{22}}\epsilon\left(\frac{\alpha_{12}}{\langle N_2\rangle} + \frac{\alpha_{21}}{\langle N_1\rangle}\right)}^{interconversion\ noise}, \tag{37}$$

with

$$\epsilon = \left(\frac{H_{11}}{\tau_1} + \frac{H_{22}}{\tau_2} - \frac{H_{21}}{\tau_1}\frac{H_{12}}{H_{22}} - \frac{H_{12}}{\tau_2}\frac{H_{21}}{H_{11}}\right)^{-1}.$$

Because $V_{12} < 0$ even if $H_{21} < 0$ when $g_1 \in [0,0.022]$, it is the negative correlation between the fluctuations in species A and B. It is found from Eq. (35) that the correlation V_{12} is determined by the intrinsic fluctuations in two species $(\langle N_i\rangle H_{ii})^{-1}(i = 1,2)$, the mutual interactions α_{12},α_{21}, the susceptibilities $H_{ij}(i,j = 1,2)$, and the average lifetimes $\tau_i(i = 1,2)$.

Equations (33) and (34) show that the noises have a correlated global component through V_{ij} [Eq. (35)] modulated by the growth fashion. The interconversion between different states provides a systemic fluctuation environment in this cascade. Equations (36) and (37) show that total noise of each species V_{ii} can be decomposed into intrinsic noise, transmitted noise, and interconversion noise. It is found that the intrinsic noise includes a pure intrinsic noise and an added one. The existence of an added part in intrinsic noise is unexpected, which differs from that of the gene regulatory networks [19] where there is no added part. The pure intrinsic noise $(\langle N_i\rangle H_{ii})^{-1}$ arises from low number of species and depends on both the average number of species $\langle N_i\rangle$ and how systematic adjustments (rate H_{ii}/τ_i) quench spontaneous fluctuations (rate $1/\tau_i$) [25]. But the added part in intrinsic noise depends on the interconversion between two species and the growth fashion. The transmitted noise comes from the intrinsic noise of other species. The interconversion noise originates from the transitions between different states. All noises (except pure intrinsic noise) depend on the logarithmic gains, the average lifetimes, and the interconversions.

B. Effects of MGR g_1 on fluctuations and noise propagation in two species

Under the initial condition $N_1(0) = N_2(0) = 20$, Fig. 2(a) shows that the populations of species A and B can reach steady states (or homeostasis) as time goes on. This equilibrium is attained by regulating each proliferation rate of two species with logistic growth feedbacks. Meanwhile, the steady states of species A and B are changed with the change of systemic parameters, seeing Eqs. (24) and (25).

The stationary populations as a function of MGR g_1 with $g_1 \in [0,0.24]$ are presented in Fig. 2(b). For a given value of

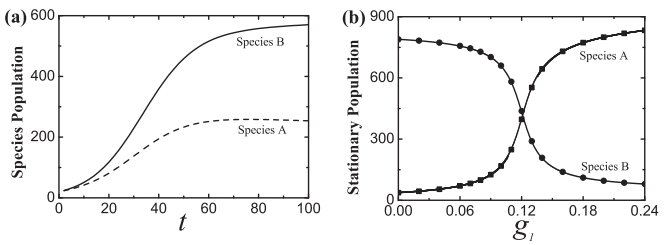

FIG. 2. (a) Time courses of species A and B with the initial conditions $N_1(0) = N_2(0) = 20$ at MGR $g_1 = 0.1$. (b) Stationary populations of species A and B as a function of MGR g_1 as ITR $s_1 = 0.001$: Lines are theoretical predictions with Eqs. (24) and (25), and solid markers are from simulations using the Gillespie method [39]. The other parameter values are given in the text. All the parameters are dimensionless.

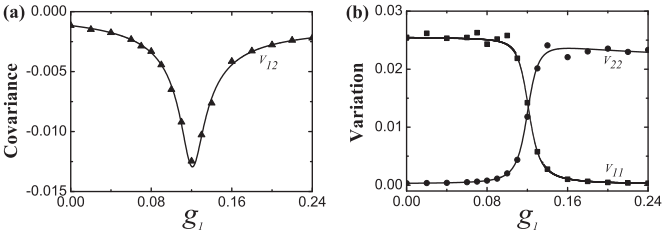

FIG. 3. Effects of MGR g_1 on (a) the normalized covariance V_{12} and (b) the normalized variations $V_{ii}(i = 1,2)$ as ITR $s_1 = 0.001$. Lines are theoretical predictions with the definition of $V_{ij}(i, j = 1,2)$, in which the detailed expressions of **C** are given by Eqs. (26) and (28). Solid markers are from simulations using the Gillespie method [39]. The other parameter values are given in the text. All the parameters are dimensionless.

the carrying capacity $N_0 = 1000$, the stationary population of species A is increased as a sigmoid shape with the increasing of g_1, while that of species B is decreased as a reversed sigmoid shape. Moreover, the stationary populations of species A and B exhibit an approximately threshold behavior as a function of g_1, and the threshold is around $g_1 = 0.121$. That is, the reproductions of species A and B can be classified into three regimens: *controlled* ($g_1 \ll 0.121$), *crossover* ($g_1 \sim 0.121$), and *controlled* ($g_1 \gg 0.121$). The threshold behaviors of the stationary populations of both species A and B found here are similar to that of post-transcriptional gene regulation by the small noncoding RNA [27,40–42].

The effects of MGR g_1 on the normalized covariance $V_{12} = C_{12}/(\langle N_1\rangle\langle N_2\rangle)$ is given in Fig. 3(a). It is found that there is a minimum for the correlation between species A and B when $g_1 = 0.121$, which exactly equals to the value of MGR g_2. It means that the larger the discrepancy between the proliferation capacities of species A and B, the stronger the correlation between their fluctuations. Moreover, the correlation was decreased with the increasing of g_1 when $g_1 < g_2$, while it increased when $g_1 > g_2$. Figure 3(b) gives the effects of g_1 on the normalized variations $V_{ii} = C_{ii}/\langle N_i\rangle^2 (i = 1,2)$. It shows that the fluctuation in species A displays a reverse sigmoidal response to the changes of g_1, while that in species B exhibits a sigmoidal response. Such a inverse behavior can be attributed to the negative correlation between the fluctuations in species A and B.

The effects of MGR g_1 on noise propagation are discussed by using Eqs. (36) and (37). With the increase of MGR g_1, Fig. 4(a) shows that the pure intrinsic noise in species A is very large at beginning and then decreases rapidly in the crossover

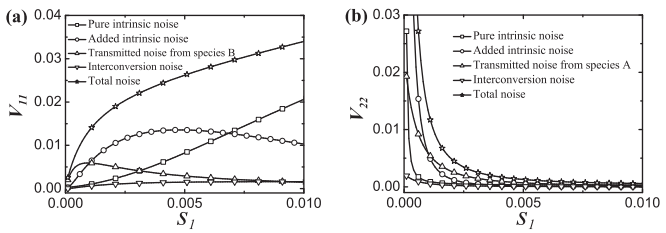

FIG. 4. Effects of MGR g_1 on noise propagations in bacterial community, $s_1 = 0.001$. All the parameters are dimensionless.

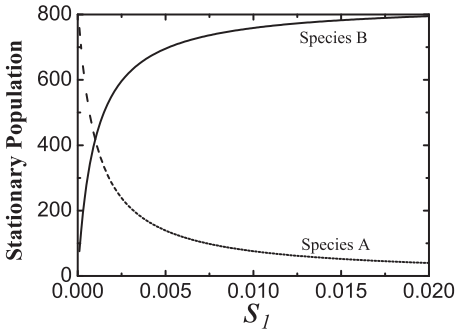

FIG. 5. Stationary populations of species A and B as a function of ITR s_1 as MGR $g_1 = 0.121$. All the parameters are dimensionless.

region due to the rapidly increasing of its average number [see Fig. 2(b)] and, finally, reaches a constant. The added intrinsic noise and transmitted noise in species A increase first, reach a maximum, and then decrease to a constant. The total noise of species A is decreased in a reversed sigmoid shape, and it is mainly determined by its intrinsic noise and the transmitted noise from species B since the interconversion noise is very small. The variation of each decomposed noise of species B is opposite to that of species A as shown by Fig. 4(b), and the total noise of species B is mainly determined by its intrinsic noise and the transmitted noise from species A.

C. Effects of ITR s_1 on fluctuations and noise propagation in two species

The stationary populations as a function of ITR s_1 with $s_1 \in [0,0.02]$ are presented in Fig. 5. Here the MGR of species A is taken to be equal to that of species B, i.e., $g_1 = g_2 = 0.121$. It is found that the stationary population of species A is decreased rapidly with the increasing of s_1 at first and then reaches a constant, whereas the stationary population of species B increases at first and then reaches a constant. Moreover, the stationary populations of species A and B also exhibit an approximately threshold behavior, and the threshold is around $s_1 = 0.001$.

The effects of ITR s_1 on the normalized covariance $V_{12} = C_{12}/(\langle N_1\rangle\langle N_2\rangle)$ is given in Fig. 6(a). We can observe that it is a negative correlation between the fluctuations in species A

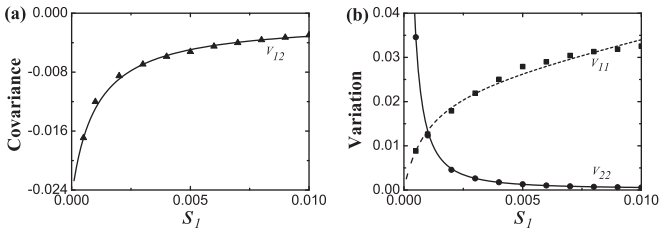

FIG. 6. Effects of ITR s_1 on (a) the normalized covariance V_{12} and (b) the normalized variations $V_{ii}(i = 1,2)$ as MGR $g_1 = 0.121$. Lines are theoretical predictions with the definition of $V_{ij}(i, j = 1,2)$, in which the detailed expressions of **C** are given by Eqs. (26) and (28). Solid markers are from simulations using the Gillespie method [39]. The other parameter values are given in the text. All the parameters are dimensionless.

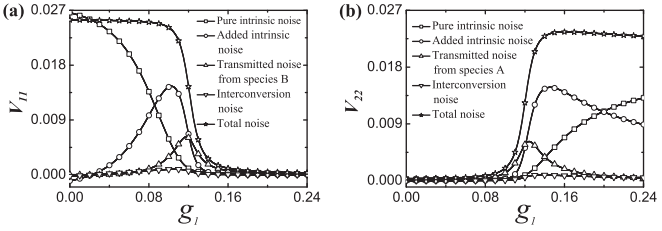

FIG. 7. Effects of ITR s_1 on noise propagations in bacterial community, $g_1 = 0.121$. All the parameters are dimensionless.

and B. Moreover, the correlation is increased monotonically before reaching a constant with the increasing of s_1. Figure 6(b) gives the effects of s_1 on the normalized variations $V_{ii} = C_{ii}/\langle N_i\rangle^2 (i = 1,2)$. It shows that the fluctuation in species A is increased monotonically with the increasing of s_1, while that in species B is decreased. Such an inverse behavior can be attributed to the negative correlation between fluctuations in two species.

The effects of ITR s_1 on noise propagation are discussed by using Eqs. (36) and (37). It can be found from Fig. 7(a) that the pure intrinsic noise of species A is almost-linearly increased since the stationary population of species A is rapidly decreased with the increasing of s_1 (see Fig. 5). The change of interconversion noise is not obvious. However, there is a maximum value for added intrinsic noise and transmitted noise. Thus the total noise of species A is increased nonlinearly and mainly determined by its intrinsic noise and the transmitted noise from species B. Figure 7(b) shows that four decomposed noises of species B are decreased with the increasing of ITR s_1, and the total noise of species B is mainly determined by its intrinsic noises and the transmitted noise from species A.

V. FLUCTUATIONS AND NOISE PROPAGATION IN THE UNIDIRECTIONAL TRANSITION CASCADE

A. Model and noise propagation formulae

Consider a model of differentiations of cell states (including three states) in a colonic crypt [17]. This is a case of a unidirectional phenotypic transition cascade [see Fig. 8) with the second regulation mechanism. It can be seen that the stem cells (SCs) are the top phenotype, and the transit amplifying cells (TACs) and fully differentiated cells (FDCs) are the downstream phenotypes. The time evolutions of SCs, TACs, and FDCs in a normal colonic crypt with a saturating feedbacks mechanism [17] are written as

$$\frac{dN_1}{dt} = a_1 N_1 - b_1 N_1 - \alpha_{12} N_1, \tag{38}$$

$$\frac{dN_2}{dt} = a_2 N_2 - b_2 N_2 + \alpha_{12} N_1 - \alpha_{23} N_2, \tag{39}$$

$$\frac{dN_3}{dt} = -b_3 N_3 + \alpha_{23} N_2, \tag{40}$$

where N_1, N_1, N_3 are the number of SCs, TACs, and FDCs, respectively. In this model, the self-proliferation rates for the three cell states are a_1 with MGR $g_1 = a_1$ for SCs, a_2 with MGR $g_2 = a_2$ for TACs, and $g_3 = a_3 = 0$ for FDCs. The transition rates among the different phenotypes

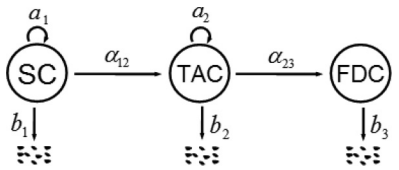

FIG. 8. The unidirectional phenotypic transition cascade. A schematic diagram of differentiations from SCs to TACs and then to FDCs in a colonic crypt.

are $\alpha_{12} = s_1[1 + k_0 N_1/(1 + m_0 N_1)]$ with ITR s_1 and $\alpha_{23} = s_2[1 + k_1 N_2/(1 + m_1 N_2)]$ with ITR s_2, in which k_i and m_i are non-negative constants, where k_i represents the speed of response of the feedback and m_i represents feedback saturation. As $m_0 = m_1 = 0$, then $\alpha_{12} = s_1(1 + k_0 N_1)$ and $\alpha_{23} = s_2(1 + k_1 N_2)$, the feedback mechanism corresponds to a linear feedback model studied in Ref. [43]. Here we take the dimensionless parameters $a_2 = 0.35$, $b_1 = b_2 = 0.1$, $b_3 = 0.139$, $s_2 = 0.3$, $k_0 = 0.4$, $m_0 = 0.1$, $k_1 = 0.001$, and $m_1 = 0.0004$ [17,28].

The concentration forms of the macroscopic rate equations Eqs. (38)–(40) are

$$\frac{dx_1}{dt} = a_1 x_1 - b_1 x_1 - \alpha_{12} x_1, \tag{41}$$

$$\frac{dx_2}{dt} = a_2 x_2 - b_2 x_2 + \alpha_{12} x_1 - \alpha_{23} x_2, \tag{42}$$

$$\frac{dx_3}{dt} = -b_3 x_3 + \alpha_{23} x_2. \tag{43}$$

The steady states are obtained as follows:

$$N_1^s = \Omega x_1^s = \frac{\beta_1}{s_1 k_0 - m_0 \beta_1}, \tag{44}$$

$$N_2^s = \Omega x_2^s = \frac{\beta_2 + m_1\kappa + \sqrt{(\beta_2 - m_1\kappa)^2 + 4 s_2 k_1 \kappa}}{2(s_2 k_1 - m_1 \beta_2)}, \tag{45}$$

$$N_3^s = \Omega x_3^s = \frac{s_2 N_2^s}{b_3}\left(1 + \frac{k_1 N_2^s}{1 + m_1 N_2^s}\right), \tag{46}$$

with

$$\beta_1 = a_1 - b_1 - s_1,$$
$$\beta_2 = a_2 - b_2 - s_2,$$
$$\kappa = \alpha_{12} N_1^s = (\beta_1 + s_1) N_1^s.$$

Here β_1 and β_2 denote the inherent net (per-capita) growth rates of SCs and TACs, respectively. κ is the stem-cell differentiation rate at the steady state. Equations (44)–(46) show that the steady states of SCs, TACs, and FDCs change with changes in systemic parameters.

According to the linear stability analysis, ITR of SCs s_1 can be determined as

$$\frac{a_1 - b_1}{1 + k_0/m_0} < s_1 < a_1 - b_1.$$

For the normal physiological condition, the number of SCs per crypt is small in a colonic crypt, meanwhile, the population of each phenotypic state (SCs, TACs, and FDCs) must maintain the stationary level.

Because the self-proliferation rates $a_i(i = 1,2,3)$ and the death rates $b_i(i = 1,2,3)$ are constant in this model, Eqs. (10) and (11) can be simplified as

$$C_{ii} = \frac{\sum_{j\neq i} C_{ij}\frac{\partial}{\partial x_j}(\alpha_{ji}x_j) + \Omega\left(a_i x_i + \sum_{j\neq i}\alpha_{ji}x_j\right)}{\frac{1}{x_i}\sum_{j\neq i}\alpha_{ji}x_j + x_i\frac{\partial}{\partial x_i}\sum_{j\neq i}\alpha_{ij}},$$

$$C_{ik} = \frac{\sum_{j\neq k} C_{ij}\frac{\partial}{\partial x_j}(\alpha_{jk}x_j) + \sum_{j\neq i} C_{kj}\frac{\partial}{\partial x_j}(\alpha_{ji}x_j) - \Omega(\alpha_{ik}x_i + \alpha_{ki}x_k)}{\frac{1}{x_i}\sum_{j\neq i}\alpha_{ji}x_j + \frac{1}{x_k}\sum_{j\neq k}\alpha_{jk}x_j + x_i\frac{\partial}{\partial x_i}\sum_{j\neq i}\alpha_{ij} + x_k\frac{\partial}{\partial x_k}\sum_{j\neq k}\alpha_{kj}}, \quad \text{for} \quad k \neq i.$$

The stationary population number can be replaced by its mean number, i.e., $N_i^s \equiv \langle N_i\rangle (i = 1,2,3)$. Based on the kinetics described in Eqs. (41)–(43), we have

$$C_{11} = \frac{a_1\langle N_1\rangle}{\beta_1 - \frac{m_0}{s_1k_0}\beta_1^2}, \tag{47}$$

$$C_{22} = \frac{\left(s_1 + 2\beta_1 - \frac{m_0}{s_1k_0}\beta_1^2\right)C_{12} + a_2\langle N_2\rangle + \kappa}{\omega_1}, \tag{48}$$

$$C_{33} = \frac{\omega_2 C_{23}}{b_3} + \langle N_3\rangle, \tag{49}$$

$$C_{12} = C_{12} = \frac{\left(s_1 + 2\beta_1 - \frac{m_0}{s_1k_0}\beta_1^2\right)C_{11} - \kappa}{\beta_1 - \frac{m_0}{s_1k_0}\beta_1^2 + \omega_1}, \tag{50}$$

$$C_{13} = C_{31} = \frac{\omega_2 C_{12}}{b_3 + \beta_1 - \frac{m_0}{s_1k_0}\beta_1^2}, \tag{51}$$

$$C_{23}{=}C_{32}{=}\frac{\left(s_1 + 2\beta_1 - \frac{m_0}{s_1k_0}\beta_1^2\right)C_{13} + \omega_2 C_{22} - b_3\langle N_3\rangle}{b_3 + \omega_1}. \tag{52}$$

with

$$\omega_1 = \beta_2 + \frac{2\kappa}{\langle N_2\rangle} - \frac{m_1}{s_2k_1}\left(\beta_2 + \frac{\kappa}{\langle N_2\rangle}\right)^2,$$

$$\omega_2 = s_2 + \beta_2 + \omega_1.$$

Taking into account the constants of both the self-proliferation rates $a_i(i = 1,2,3)$ and the death rates $b_i(i = 1,2,3)$, Eqs. (15) and (16) can be simplified as

$$H_{ii} = \frac{\sum_{j\neq i}\alpha_{ji}N_j + N_i^2\frac{\partial}{\partial N_i}\left(\sum_{j\neq i}\alpha_{ij}\right)}{a_iN_i + \sum_{j\neq i}\alpha_{ji}N_j},$$

$$H_{ik} = -\frac{N_i}{a_kN_k + \sum_{j\neq k}\alpha_{jk}N_j}\frac{\partial}{\partial N_i}(\alpha_{ik}N_i), \quad \text{for} \quad k \neq i.$$

Therefore, $H_{13} = H_{21} = H_{31} = H_{32} = 0$, $H_{33} = 1$, and

$$H_{11} = \frac{\beta_1}{a_1}\left(1 - \frac{m_0}{s_1k_0}\beta_1\right), \tag{53}$$

$$H_{22} = \frac{\beta_2 + \frac{2\kappa}{\langle N_2\rangle} - \frac{m_1}{s_2k_1}\left(\beta_2 + \frac{\kappa}{\langle N_2\rangle}\right)^2}{a_2 + \frac{\kappa}{\langle N_2\rangle}}, \tag{54}$$

$$H_{12} = -\frac{s_1 + 2\beta_1 - \frac{m_0}{s_1k_0}\beta_1^2}{a_2\frac{\langle N_2\rangle}{\langle N_1\rangle} + s_1 + \beta_1}, \tag{55}$$

$$H_{23} = -\frac{s_2 + 2\left(\beta_2 + \frac{\kappa}{\langle N_2\rangle}\right) - \frac{m_1}{s_2k_1}\left(\beta_2 + \frac{\kappa}{\langle N_2\rangle}\right)^2}{s_2 + \beta_2 + \frac{\kappa}{\langle N_2\rangle}}. \tag{56}$$

It can be shown that $H_{11}, H_{22} > 0$ and $H_{12}, H_{23} < 0$.

To study the noise propagation in three phenotypic states in colonic crypt, expanding the theoretical formulas Eqs. (18) and (19) with $V_{ij} = V_{ji}(i, j = 1,2,3)$ here, we can obtain

$$V_{11} = \frac{1}{\langle N_1\rangle H_{11}}, \tag{57}$$

$$V_{22} = \frac{1}{\langle N_2\rangle H_{22}} - \frac{H_{12}}{H_{22}}V_{12}, \tag{58}$$

$$V_{33} = \frac{1}{\langle N_3\rangle H_{33}} - \frac{H_{23}}{H_{33}}V_{23}, \tag{59}$$

$$V_{12} = V_{21} = -\frac{H_{12}V_{11}/\tau_2 + \alpha_{12}/\langle N_2\rangle}{H_{11}/\tau_1 + H_{22}/\tau_2}, \tag{60}$$

$$V_{13} = V_{31} = -\frac{H_{23}/\tau_3}{H_{11}/\tau_1 + H_{33}/\tau_3}V_{12}, \tag{61}$$

$$V_{23} = V_{32} = -\frac{H_{12}V_{13}/\tau_2 + H_{23}V_{22}/\tau_3 + \alpha_{23}/\langle N_3\rangle}{H_{22}/\tau_2 + H_{33}/\tau_3}, \tag{62}$$

where the average lifetimes are $\tau_1 = 1/a_1$, $\tau_2 = 1/(b_2 + \alpha_{23})$, $\tau_3 = 1/b_3$, respectively. Solving these equations for V_{ij}, then

$$V_{11} = \overbrace{\frac{1}{\langle N_1\rangle H_{11}}}^{\textit{Intrinsic noise in SCs}}, \tag{63}$$

$$V_{22} = \overbrace{\frac{1}{\langle N_2\rangle H_{22}}}^{\textit{Intrinsic noise in TACs}} + \overbrace{V_{11}\left(\frac{H_{12}}{H_{22}}\right)^2\frac{H_{22}/\tau_2}{H_{11}/\tau_1 + H_{22}/\tau_2}}^{\textit{Transmitted noise from SCs}} + \overbrace{\frac{H_{12}}{H_{22}}\frac{\alpha_{12}/\langle N_2\rangle}{H_{11}/\tau_1 + H_{22}/\tau_2}}^{\textit{Conversion noise between SCs and TACs}}, \tag{64}$$

$$V_{33} = \overbrace{\frac{1}{\langle N_3\rangle H_{33}}}^{Intrinsic\ noise\ in\ FDCs} + \overbrace{V_{11}\left(\frac{H_{12}}{H_{22}}\right)^2\left(\frac{H_{23}}{H_{33}}\right)^2 \frac{H_{22}/\tau_2}{H_{11}/\tau_1 + H_{22}/\tau_2}\frac{H_{22}/\tau_2}{H_{22}/\tau_2 + H_{33}/\tau_3}\frac{H_{33}/\tau_3}{H_{11}/\tau_1 + H_{33}/\tau_3}}^{Transmitted\ noise\ from\ SCs}$$
$$+ \overbrace{V_{22}\left(\frac{H_{23}}{H_{33}}\right)^2 \frac{H_{33}/\tau_3}{H_{22}/\tau_2 + H_{33}/\tau_3}}^{Transmitted\ noise\ from\ TACs} + \overbrace{\frac{H_{23}}{H_{33}}\frac{\alpha_{23}/\langle N_3\rangle}{H_{22}/\tau_2 + H_{33}/\tau_3}}^{Conversion\ noise\ between\ TACs\ and\ FDCs}$$
$$+ \overbrace{\frac{H_{12}}{H_{22}}\left(\frac{H_{23}}{H_{33}}\right)^2 \frac{H_{22}/\tau_2}{H_{22}/\tau_2 + H_{33}/\tau_3}\frac{H_{33}/\tau_3}{H_{11}/\tau_1 + H_{33}/\tau_3}\frac{\alpha_{12}/\langle N_2\rangle}{H_{11}/\tau_1 + H_{22}/\tau_2}}^{Conversion\ noise\ between\ SCs\ and\ TACs}, \tag{65}$$

$$V_{12} = V_{21} = -V_{11}\frac{H_{12}}{H_{22}}\frac{H_{22}/\tau_2}{H_{11}/\tau_1 + H_{22}/\tau_2} - \frac{\alpha_{12}/\langle N_2\rangle}{H_{11}/\tau_1 + H_{22}/\tau_2}, \tag{66}$$

$$V_{13} = V_{31} = -V_{12}\frac{H_{23}}{H_{33}}\frac{H_{33}/\tau_3}{H_{11}/\tau_1 + H_{33}/\tau_3}, \tag{67}$$

$$V_{23} = V_{32} = -V_{13}\frac{H_{12}}{H_{22}}\frac{H_{22}/\tau_2}{H_{22}/\tau_2 + H_{33}/\tau_3} - V_{22}\frac{H_{23}}{H_{33}}\frac{H_{33}/\tau_3}{H_{22}/\tau_2 + H_{33}/\tau_3} - \frac{\alpha_{23}/\langle N_3\rangle}{H_{22}/\tau_2 + H_{33}/\tau_3}. \tag{68}$$

It can be shown that $V_{12}, V_{13}, V_{23} > 0$, it is a positive correlation between any two fluctuations in three phenotypic states. Meanwhile, Eq. (66) shows that V_{12} is determined by the intrinsic fluctuation in SCs V_{11}, the relative susceptibility H_{12}/H_{22}, the time-averaging $\frac{H_{22}/\tau_2}{H_{11}/\tau_1+H_{22}/\tau_2}$, and the direct interaction between SCs and TACs α_{12}. It is found from Eq. (67) that the correlation can be transmitted from SCs to FDCs by TACs, though there is no direct interaction between them. The transmitted correlation V_{13} also can influence the correlation between TACs and FDCs V_{23}, seeing Eq. (68). In addition, V_{23} is dependent on the intrinsic fluctuation in TACs V_{22} and the direct interaction between TACs and FDCs α_{23}.

Equations (58) and (59) show that a fluctuation environment in each downstream state is provided by upstream states through the correlation between fluctuations V_{ij} modulated by the feedback mechanisms. The noise in upstream states can propagate in this cascade. For the top phenotype, SCs, Eq. (63) shows that the total noise in SCs is only a pure intrinsic noise, and there is no random fluctuation environment provided by other compartments. Eqs. (64) and (65) show that the total noises of TACs and FDCs can be decomposed into intrinsic noise, transmitted noise, and conversion noise. The pure intrinsic noise $(\langle N_i\rangle H_{ii})^{-1}$ of TACs or FDCs depends on its low numbers. The transmitted noise in TACs comes from the intrinsic noise of SCs, and the conversion noise in TACs is caused by the transition from SCs to TACs. However, the transmitted noise in FDCs includes two parts, one is the intrinsic noise of SCs and the other is the total noise of TACs. Meanwhile, the conversion noise in FDCs is also composed of two parts: One comes from the transition from TACs to FDCs and the other originates from the transition from SCs to TACs, respectively.

B. Effects of ITR s_1 on fluctuations and noise propagation in three phenotypic states

Under the initial condition of cell populations $N_1(0) = N_2(0) = N_3(0) = 100$, Fig. 9(a) shows that the populations of SCs, TACs, and FDCs can reach steady states (or homeostasis) as time goes on. The above results demonstrate that the saturation feedbacks of SCs and TACs can control the switching rates and make the system maintain a stable equilibrium. Meanwhile, the steady states of SCs, TACs, and FDCs are changed with changes in systemic parameters. Only the effects of s_1 on the system are considered in the following. The stationary populations as a function of s_1 with $s_1 \in [0.15, 0.45]$ are presented in Fig. 9(b). It is shown that each stationary population decreases with the increasing of s_1. At a given value of s_1, the stationary population of FDCs is the highest and that of SCs is the lowest, which agrees with the natural physiological phenomenon.

The effects of ITR s_1 on the normalized variations $V_{ii} = C_{ii}/\langle N_i\rangle^2 (i = 1,2,3)$ and the normalized covariances $V_{ij} = C_{ij}/(\langle N_i\rangle\langle N_j\rangle)(j \neq i)$ are given in Fig. 10. It is found from Fig. 10(a) that the responses of V_{12}, V_{13}, and V_{23} to the change of the value s_1 are analogous. Each one increases monotonically with the increasing of s_1. Meanwhile, at a given value of s_1, $V_{23} > V_{12} > V_{13}$. It means that the correlation between TACs and FDCs is the strongest because FDCs are produced completely by the differentiation of TACs, while that between SCs and FDCs is the weakest since there is no direct

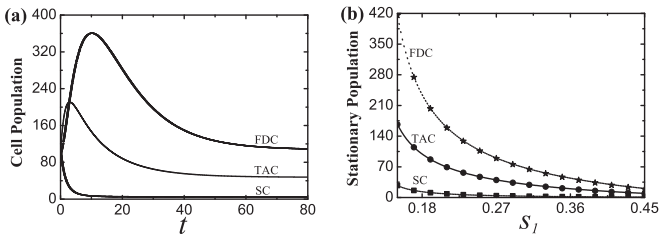

FIG. 9. (a) Time courses of SCs, TACs, and FDCs with the initial conditions $N_1(0) = N_2(0) = N_3(0) = 100$ at ITR $s_1 = 0.25$. (b) Stationary populations of SCs, TACs, and FDCs as a function of ITR s_1 as MGR $g_1 = 0.69$: Lines are theoretical predictions with Eqs. (44)–(46) and solid markers are from simulations using the Gillespie method [39]. The other parameter values are given in the text. All the parameters are measured in hours^{-1}.

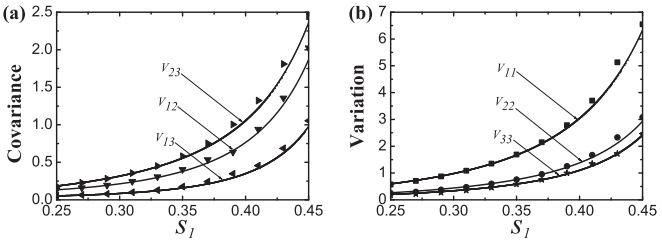

FIG. 10. Effects of ITR s_1 on (a) the normalized covariance V_{ij} and (b) the normalized variations V_{ii} as MGR $g_1 = 0.69$. Lines are theoretical predictions with the definition of $V_{ij}(i,j = 1,2,3)$, in which the detailed expressions of $\mathbf{C}$ are given by Eqs. (47)–(52). Solid markers are from simulations using the Gillespie method [39]. The other parameter values are given in the text. All the parameters are measured in hours^{-1}.

relationship between them. Due to the positive correlation between any two fluctuations in three phenotypic states, each variation increases monotonically with the increasing of s_1, shown in Fig. 10(b). Meanwhile, $V_{11} > V_{22} > V_{33}$ at a given value of s_1.

The effects of ITR s_1 on noise propagation in three cell states are discussed by using Eqs. (64) and (65). With the increasing of ITR s_1, Fig. 11 shows that both intrinsic noises and transmitted noises in TACs and FDCs are increased, but the conversion noises in TACs and FDCs are decreased. The total noise in TACs is mainly dependent on the transmitted noise from SCs, while the total noise in FDCs mainly relies on the transmitted noise from TACs and SCs.

C. Effects of MGR g_1 on fluctuations and noise propagation in three phenotypic states

The stationary populations as a function of MGR g_1 with $g_1 \in [0.25,0.50]$ are presented in Fig. 12. Here we choose $s_1 = 0.1$ when the inherent differentiation of SCs is slower than that of TACs. It is found that the stationary populations of SCs, TACs, and FDCs are increased fast with the increasing of g_1.

The effects of MGR g_1 on the normalized variations $V_{ii} = C_{ii}/\langle N_i\rangle^2 (i = 1,2,3)$ and the normalized covariances $V_{ij} = C_{ij}/(\langle N_i\rangle\langle N_j\rangle)(j \neq i)$ are given in Fig. 13. It is found from Fig. 13(a) that the responses of V_{12}, V_{13}, and V_{23} to the change of the value g_1 are analogous. Each one decreases monotonically with the increasing of g_1. Due to the positive correlation between any two fluctuations in three

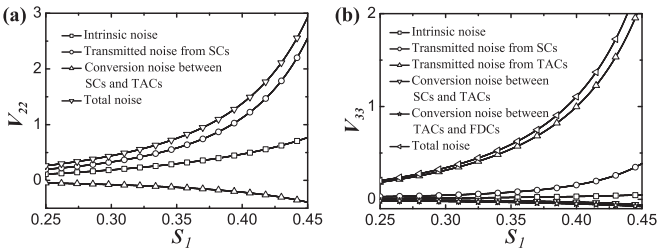

FIG. 11. Effects of ITR s_1 on noise propagations in cell states cascade in colonic crypt, $g_1 = 0.69$. All the parameters are measured in hours^{-1}.

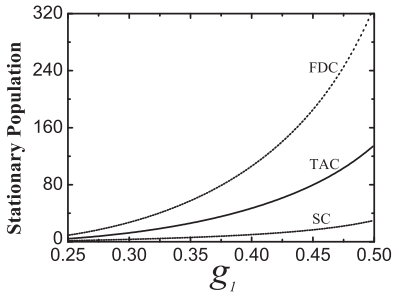

FIG. 12. Stationary populations of SCs, TACs, and FDCs as a function of MGR g_1 as ITR $s_1 = 0.1$. All the parameters are measured in hours^{-1}.

phenotypic states, each variation decreases monotonically with the increasing of g_1, shown in Fig. 13(b).

The effects of MGR g_1 on noise propagation in three cell states are discussed by using Eqs. (64) and (65). It is found from Fig. 14 that the intrinsic noises and transmitted noises in both TACs and FDCs are decreased, but the conversion noises in TACs and FDCs are increased with the increasing of MGR g_1. The total noise in TACs or FDCs mainly relies on the transmitted intrinsic noise from the upstream cell states since the intrinsic noises and the conversion noises in TACs or FDCs are comparatively small.

VI. CONCLUSIONS AND DISCUSSIONS

Understanding how noise propagates through various phenotypic transition cascades around the equilibrium state is a significant problem in populations. In this paper we started by constructing a general model of populations, the theoretical formulas for noise propagation in various phenotypic transition cascades are derived by using the linear noise approximation of master equation and the logarithmic gain. The solution V_{ii} of theoretical formulas Eqs. (18) and (19) represents the total noise in the ith phenotypic state, which may include the intrinsic noise in the ith phenotypic state, the transmitted noise from the other phenotypes, and the interconversion noise. The solution V_{ij} represents the correlation between fluctuations in the ith phenotype and in the jth phenotype.

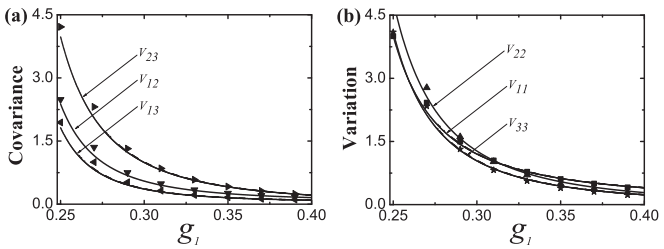

FIG. 13. Effects of MGR g_1 on (a) the normalized covariance V_{ij} and (b) the normalized variations V_{ii} as ITR $s_1 = 0.1$. Lines are theoretical predictions with the definition of $V_{ij}(i,j = 1,2,3)$, in which the detailed expressions of $\mathbf{C}$ are given by Eqs. (47)–(52). Solid markers are from simulations using the Gillespie method [39]. The other parameter values are given in the text. All the parameters are measured in hours^{-1}.

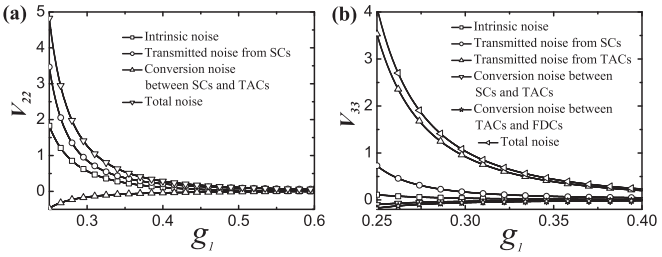

FIG. 14. Effects of MGR g_1 on noise propagations in cell states cascade in colonic crypt, $s_1 = 0.1$. All the parameters are measured in hours^{-1}.

To uncover the effects of interconversion rate between distinct phenotypes or self-proliferation rate of one phenotype on the noise propagation in various phenotypic transition cascades, we studied a model of two species with exploitative competition in a bacterial community [24] which is a case of the bidirectional phenotypic transition cascade with the first regulation mechanism, and a model of three cell compartments in a colonic crypt [17] which is a case of the unidirectional phenotypic transition cascade with the second regulation mechanism, respectively. It was found that the mechanisms of noise propagation and the effects of the interconversion or self-proliferation rate on noise propagation differ remarkably in the bidirectional and unidirectional transition cascades.

In the bidirectional cascade, the systemic random environment is provided by all phenotypes in this cascade, and the total noise of each phenotype is determined by its intrinsic noise, the transmitted noises from other phenotypes, and the interconversion noise. The existence of an added part in intrinsic noise shows a novel noise propagation mechanism, which differs from that of gene regulatory networks [19] in which there is no added part. In the unidirectional cascade, however, the random environment for each downstream phenotype is provided only by the upstream phenotypes. The total noise of each phenotype (except the top phenotype) is mainly determined by the transmitted noises from other phenotypes, rather than by its intrinsic noise. It should be pointed out that above theoretical results are coincident with those obtained by the Gillespie algorithm [39] in the region of given parameter values as shown in Figs. 2(b), 3, 6, 9(b), 10, and 13.

Although our theoretical formulas Eqs. (18) and (19) had been applied to study fluctuations and noise propagation in the model of bacterial community with exploitative competition [24] and the model of differentiations of cell states in a colonic crypt [17], the theoretical formulas can also be applied to investigate the noise propagation in other transition cascade (or interaction network) models since the conversion rates between distinct phenotypes and self-proliferation (or self-growth) rate of each phenotype (or component) in the starting general model Eq. (1) are assumed as arbitrary functions of subpopulations. Here we provide some applicable models in which the self-growth rate of each component and the conversion rates between distinct components are known. For example, (i) for the case of $\alpha_{ij} = 0$ (i.e., no interconversion between distinct components), the self-growth rate and death rate of each component are $a_1 = \frac{\beta_1 n_0/K_{11}}{1+n_1/K_{11}+n_2/K_{12}} + \frac{l}{n_1}$, $a_2 = \frac{\beta_2 n_1/(K_2 n_2)}{1+n_1/K_{21}+(n_2/K_{22})^2}$, $b_1 = \alpha_1$, and $b_2 = \alpha_2$ in the model of interactions between genes and proteins [21]; $a_1 = \lambda_1 - \lambda_3$, $a_2 = \lambda_2 + 2\lambda_3$, $b_1 = 0$, and $b_2 = \Gamma$ in the single progenitor cell model for skin cell proliferation [28]; and $a_1 = \alpha_s/S$, $a_2 = \alpha_m/M$, $b_1 = \beta_s + kM$, and $b_2 = \beta_m + kS$ in the model of post-transcriptional gene regulation by small noncoding RNA [27,40] where the sRNA and its target gene mRNA degrade together, and both per-capital death rates are not constant. (ii) For the case of $\alpha_{ij} \neq 0$, we have $a_1 = \mu_n$, $b_1 = 0$, $a_2 = \mu_p$, $b_2 = 0$, $\alpha_{12} = a$, and $\alpha_{21} = b$ in the model of *E. coli* persistence [12]. By the way, we can obtain the theoretical results in the model of gene-regulatory networks [25] by solving Eqs. (18) and (19) through setting the conversion rates $\alpha_{12} = \alpha_{21} = 0$.

The goal of this paper is to investigate the fluctuation and noise propagation in various phenotypic transition cascades around the steady state of subpopulations. Our results show that the noise propagation in various phenotypic cascades depends mainly on the mechanisms of interconversion between distinct phenotypes, which accords with the biological experimental findings that a rapid progression toward equilibrium proportions of human breast cells in various states is not due to differential self-growth rates of cells in the basal, stemlike, or luminal states but rather to interconversion between states [16]. Unfortunately, the theoretical formulas Eqs. (18) and (19) cannot be applied to the dynamics of phenotypic equilibrium proportions in breast cancer cell lines, and there are two insuperable obstacles in the application of our theoretical formulas: (i) there is no experimental data about fluctuations and noise propagation in the phenotypic transition cascade of breast cancer. In fact, Ref. [16] showed that subpopulations of cells purified for a given phenotypic state return towards equilibrium *proportions* over time, and these observations were explained by a Markov model in which cells transition stochastically between different states; (ii) one cannot obtain an analytical steady state of subpopulations from the model of Ref. [16].

It should be emphasized that the theoretical formulas Eqs. (18) and (19) for noise propagation were derived at the cellular level [see Eq. (1)], and the bidirectional cascade and the unidirectional cascade are two basic ways in phenotypic transitions. The differentiations from SCs to TACs and then to FDCs in a normal colonic crypt (as shown in Fig. 8) forms the unidirectional phenotypic transition cascade. Many experimental data showed that the number of stem cells (SCs) in a normal (or healthy) colonic crypt is often very limited. For instance, Potten and Loeffler [44] reported that the numbers are discrepant due to different measurements or considerations and concluded they may be approximately 4–40. Cai *et al.* [45] showed that the number of stem cells is between 5 and 10. By using chemical mutagenesis, radiation regeneration, or other experimental techniques, the experimental data from Refs. [46–50] demonstrated that the number of stem cells is about 4–6. Therefore, the highly relative intrinsic fluctuations in populations of SCs, TACs, and FDCs cannot be neglected due to the very small number of SCs. However, it seems very difficult to quantitatively compare our theoretical results with the experimental data. There are a few very different experimental data only referring to the number of SCs, while any real data about the numbers of TACs and FDCs could not be found in published papers up to now. In addition, for

different fates of cells, Momiji and Monk [51] investigated the impact of local feedback loops in a model of lateral inhibition based on the Notch signaling pathway, elucidating the roles of intracellular and intercellular delays in controlling the overall system behavior. The bidirectional phenotypic transition cascade shown in Fig. 1 is a typical cascade motif, thus, it would be highly interesting to investigate the effects of time delays of conversion rates on the fluctuation and noise propagation in our future works.

The conversion between different phenotypes plays a very important role in fluctuations of phenotypic transition cascades. It leads to an added intrinsic noise in the bidirectional phenotypic transition cascade. The intrinsic noise and the conversion noise can propagate in both bidirectional and unidirectional phenotypic transition cascades. Therefore, it is necessary to understand and consider the effects of conversion and noise propagation on natural phenotypic transition cascades.

ACKNOWLEDGMENTS

This work was supported by the National Natural Science Foundation of China under 11105059 (X.Z.), 11105058 (L.J.Y.), 20201260169 (A.B.L.), 11175068 and 11474117 (Y.J.), the CCNU12A01011 (X.Z.), and the Technology Creative Project of Excellent Middle and Young Team of Hubei Province under T201204 (Q.M.P.).

[1] H. R. Bonifield and K. T. Hughes, J. Bacteriol. **185**, 3567 (2003).
[2] N. Q. Balaban, J. Merrin, R. Chait, L. Kowalik, and S. Leibler, Science **305**, 1622 (2004).
[3] D. B. Kearns, F. Chu, R. Rudner, and R. Losick, Mol. Microbiol. **52**, 357 (2004).
[4] I. R. Henderson and S. E. Jacobsen, Nature (London) **447**, 418 (2007).
[5] V. K. Rakyan, S. Chong, M. E. Champ, P. C. Cuthbert, H. D. Morgan, K. V. K. Luu, and E. Whitelaw, Proc. Natl. Acad. Sci. USA **100**, 2538 (2003).
[6] G. M. Suel, J. Garcia-Ojalvo, L. M. Liberman, and M. B. Elowitz, Nature (London) **440**, 545 (2006).
[7] G. M. Suel, R. P. Kulkarni, J. Dworkin, J. Garcia-Ojalvo, and M. B. Elowitz, Science **315**, 1716 (2007).
[8] M. Thattai and A. van Oudenaarden, Genetics **167**, 523 (2004).
[9] S. Di Talia, J. M. Skotheim, J. M. Bean, E. D. Siggia, and F. R. Cross, Nature (London) **448**, 947 (2007).
[10] E. Kussell and S. Leibler, Science **309**, 2075 (2005).
[11] M. Salathé, J. V. Cleve, and M. W. Feldman, Genetics **182**, 1159 (2009).
[12] E. Kussell, R. Kishony, N. Q. Balaban, and S. Leibler, Genetics **169**, 1807 (2005).
[13] E. Kussell, S. Leibler, and A. Grosberg, Phys. Rev. Lett. **97**, 068101 (2006).
[14] M. Acar, J. T. Mettetal, and A. van Oudenaarden, Nat. Genet. **40**, 471 (2008).
[15] Y. Wakamoto, N. Dhar, R. Chait, K. Schneider, F. Signorino-Gelo, S. Leibler, and J. D. McKinney, Science **339**, 91 (2013).
[16] P. B. Gupta, C. M. Fillmore, G. Jiang, S. D. Shapira, K. Tao, C. Kuperwasser, and E. S. Lander, Cell **146**, 633 (2011).
[17] M. D. Johnston, C. M. Edwards, W. F. Bodmer, P. K. Maini, and S. J. Chapman, Proc. Natl. Acad. Sci. USA **104**, 4008 (2007).
[18] M. Thattai and A. van Oudenaarden, Biophys. J. **82**, 2943 (2002).
[19] J. M. Pedraza and A. van Oudenaarden, Science **307**, 1965 (2005).
[20] G. Rieckh and G. Tkacik, Biophys. J. **106**, 1194 (2014).
[21] G. Hornung and N. Barkai, PloS Comput. Biol. **4**, e8 (2008).
[22] N. G. van Kampen, *Stochastic Processes in Physics and Chemistry, 2nd ed.* (Elsevier, Amsterdam, 1997).
[23] T. Brett and T. Galla, Phys. Rev. Lett. **110**, 250601 (2013).
[24] J. Mao, A. E. Blanschard, and T. Lu, ACS Synth. Biol. ACS Synth. Biol. **4**, 240 (2015).
[25] J. Paulsson, Nature (London) **427**, 415 (2004).
[26] J. Paulssson, Phys. Life. Rev. **2**, 157 (2005).
[27] Y. Jia, W. H. Liu, A. B. Li, L. J. Yang, and X. Zhan, Biophys. Chem. **143**, 60 (2009).
[28] P. B. Warren, Phys. Rev. E **80**, 030903(R) (2009).
[29] Y. Jia and J. R. Li, Phys. Rev. Lett. **78**, 994 (1997).
[30] J. Elf and M. Ehrenberg, Genome Res. **13**, 2475 (2003).
[31] P. Thomas, A. V. Straube, and R. Grima, BMC Syst. Biol. **6**, 39 (2012).
[32] M. A. Savageau, *Biochemical Systems Analysis: A Study of Function and Design in Molecular Biology* (Addison-Wesley, Reading, MA, 1976).
[33] A. Goldbeter and D. E. Koshland, Q. Rev. Biophys. **15**, 555 (1982).
[34] R. Heinrich and S. Schuster, *The Regulation of Cellular Systems* (Champman & Hall, New York, 1996).
[35] M. Scott, B. Ingalls, and M. Kærn, Chao **16**, 026107 (2006).
[36] S. Pigolotti, C. López, and E. Hernández-García, Phys. Rev. Lett. **98**, 258101 (2007).
[37] T. Reichenbach, M. Mobilia, and E. Frey, Phys. Rev. Lett. **99**, 238105 (2007).
[38] S. Tănase-Nicola and I. Nemenman, J. R. Soc. Interface **9**, 1354 (2012).
[39] D. T. Gillespie, J. Phys. Chem. **81**, 2340 (1977).
[40] E. Levine, Z. Zhang, T. Kuhlman, and T. Hwa, PLoS Biol. **5**, e229 (2007).
[41] Y. Shimoni, G. Friedlander, G. Hetzroni, G. Niv, S. Altuvia, O. Biham, and H. Margalit, Mol. Syst. Biol. **3**, 138 (2007).
[42] E. Levine and T. Hwa, Curr. Opin. Microbiol. **11**, 574 (2008).
[43] Q. M. Pei, X. Zhan, L. J. Yang, C. Bao, W. Cao, A. B. Li, A. Rozi, and Y. Jia, Phys. Rev. E **89**, 032715 (2014).
[44] C. S. Potten and M. Loeffler, Development (Cambridge, UK) **110**, 1001 (1990).
[45] W. B. Cai, S. A. Roberts, and C. S. Potten, Int. J. Radiat. Biol. **71**, 573 (1997).
[46] C. S. Potten, C. Booth, and D. M. Pritchard, Int. J. Exp. Pathol. **78**, 219 (1997).
[47] C. S. Potten, Philos. Trans. R. Soc. London, B **353**, 821 (1998).
[48] M. Bjerknes and H. Cheng, Gastroenterology **116**, 7 (1999).
[49] E. Marshman, C. Booth, and C. S. Potten, BioEssays **24**, 91 (2002).
[50] Z. Wang, P. Matsudaira, and Z. Gong, PLoS ONE **5**, e14063 (2010).
[51] H. Momiji and N. A. M. Monk, Phys. Rev. E **80**, 021930 (2009).